Performance of the muon detector A under TIBET Ⅲ array *

LIU Cheng(刘成)[1;1)] BI Xiao-Jun(毕效军)[1] CHEN Tian-Lu(陈天禄)[2] CHEN Wen-Yi(陈文益)[1]
CUI Shu-Wang(崔树旺)[3] DANZENGLUOBU(单增罗布)[2] DING Lin-Kai(丁林恺)[1] DING Xiao-Hong(丁晓红)[2]
FENG Cun-Feng(冯存峰)[4] FENG Zhao-Yang(冯朝阳)[1] FENG Zhen-Yong(冯振勇)[5] GOU Quan-Bu(苟全补)[1]
GUO Hong-Wei(郭宏伟)[2] GUO Yi-Qing(郭义庆)[1] HE Hui-Hai(何会海)[1] HOU Zheng-Tao(侯正涛)[3]
HU Hai-Bing(胡海冰)[2] HU Hong-Bo(胡红波)[1] HUANG Jing(黄晶)[1] LI Wan-Jie(李万杰)[1,5]
JIA Huan-Yu(贾焕玉)[5] JIANG Long(姜龙)[1] KANG Ming-Ming(康明铭)[1] LE Gui-Ming(乐贵明)[1]
LEI Wen-Hua(雷文华)[2] LI Ai-Feng(李爱凤)[6,4,1] LI Hai-Jin(厉海金)[2] LIU Jin-Sheng(刘金胜)[1]
LIU Mao-Yuan(刘茂元)[2] LU Hong(卢红)[1] MENG Xian-Ru(孟宪茹)[2] QIAN Xiang-Li(钱祥利)[4]
QU Xiao-Bo(曲晓波)[1] TAN You-Heng(谭有恒)[1] WANG Hui(王辉)[1] WU Han-Rong(吴含荣)[1]
SHEN Chang-Quan(沈长铨)[1] SHEN Pei-Ruo(沈培若)[1] XUE Liang(薛良)[4] YANG Zhen(杨振)[1]
YUAN Ai-Fang(袁爱芳)[2] ZHAI Liu-Ming(翟留名)[1] ZHANG Hui-Min(张慧敏)[1]
ZHANG Ji-Long(张吉龙)[1] ZHANG Xue-Yao(张学尧)[4] ZHANG Yong(张勇)[1]
ZHANG Yi(张毅)[1] ZHANG Ying(张颖)[1] ZHOU Xun-Xiu(周勋秀)[5]

[1] Institute of High Energy Physics, Chinese Academy of Sciences, Beijing 100049, China
[2] Tibet University, Lhasa 850000, China
[3] Hebei Normal University, Shijiazhuang 050024, China
[4] Shandong University, Jinan 250100, China
[5] Southwest Jiaotong University, Chengdu 610031, China
[6] Shandong Agriculture University, Taian 271018, China

Abstract: In order to observe gamma rays in the 100 TeV energy region, the 4500 m^2 underground muon detector array using water Cherenkov technique is constructed, forming the TIBET Ⅲ+MD hybrid array. Because the showers induced by primary gamma rays contain much fewer muons than those induced by primary hadrons, significant improvement of the gamma ray sensitivity for TIBET Ⅲ+MD array is expected. In this paper, the design and performance of the MD-A detector with large Tyvek bag is reported.

Key words: TIBET Ⅲ array, muon detector, water Cherenkov, large Tyvek bag

PACS: 96.50.sd, 95.55.Ka, 29.40.Ka **DOI:** 10.1088/1674-1137/37/2/026001

1 Introduction

In 1989, Crab nebula was first detected as a TeV gamma ray source [1]. At present, the number of TeV gamma ray sources has increased rapidly and more than 100 sources have been identified. On the other hand, 1873 sources are detected in GeV energy region by the Fermi Gamma-ray Space Telescope with two years' operation [2]. The multi-wavelength observations have offered us great opportunities to study the origin and acceleration of cosmic rays.

High energy gamma rays are the best probe of the undergoing cosmic accelerators. The characteristic feature of an electron process is that the spectrum exhibits a two-component structure. The low energy one is due to the synchrotron radiation of an electron in the surrounding magnetic field while the high energy one is from inverse Compton and bremsstrahlung. The very high energy component might not be easily produced by electrons due to the fast cooling of high energy electrons and the Klein-Nishina effect of the inverse Compton scattering. Cosmic ray nuclei may generate high energy gamma rays through the decay of π^0s generated in its hadronic interaction with ambient gas. The gamma ray spectrum

Received 8 March 2012, Revised 31 March 2012

* Supported by Ministry of Science and Technology of China, National Natural Science Foundation of China (10725524, 11135010, 10875132, 11105156), Chinese Academy of Sciences (KJCX2-YW-N13, GJHZ1004, 2A20093111116010), Knowledge Innovation Fund (H85451D1U2) of IHEP, China

1) E-mail: liuc@mail.ihep.ac.cn

from the hadronic process inherits that of the cosmic ray and may extend to PeV energy or higher. Up to now, almost all available spectra observed can be described by electron processes and no source is conclusively identified as a hadronic source, neither Galactic nor extragalactic origin. Though it is a difficult task, the observation of gamma rays in 100 TeV energy region becomes very important in the search for a hadronic source.

Having advantages in both high altitude and large area, the TIBET Ⅲ array would be an ideal experiment in observing 100 TeV gamma rays if it had the discrimination power in distinguishing the gamma rays from the overwhelming cosmic ray background. To improve the sensitivity to observe celestial gamma ray sources around 100 TeV, the muon detector (MD) array using water Cherenkov technique is being built under the Tibet Air Shower (AS) array. A water Cherenkov detector has been used in many experiments, such as Super-Kamiokande, at the Pierre Auger observatory and the HAWC observatory. For different physics goals, the detectors could be designed rather differently. In this paper, the performance of muon detector A using large Tyvek bag technique is described.

2 TIBET Ⅲ array and MD array

Since 1990, the Tibet AS array has been in operation at Yangbajing (90°31′ E, 30°06′ N; 4300 m above sea level) in Tibet, China. Each counter has a plastic scintillator plate of 0.5 m^2 in area and 3 cm in thickness. It is equipped with a fast-timing (FT) 2-inch-diameter photomultiplier tube (FT-PMT, Hamamatsu H1161) and/or a wide dynamic range 1.5-inch-diameter PMT (D-PMT, Hamamatsu H3178). A 0.5 cm thick lead plate is put on the top of each counter in order to increase the counter sensitivity by converting gamma rays into electron-positron pairs in an electromagnetic shower. In the late fall of 2003, the area of the Tibet AS array was further enlarged up to 36900 m^2 as TIBET Ⅲ array which consists of 728 FT-counters (249 of them also have 1 D-PMT) and 28 D-counters [3].

The TIBET Ⅲ array has been working in a wide energy range from TeV to 100 PeV. For 100 TeV gamma ray, the angular resolution is about 0.2 degrees and the energy resolution is about 40%. During its successful operation of more than twenty years, the Tibet AS array has obtained many important physics results. In 1999, the multi-TeV gamma ray emission from Crab was detected with the Tibet AS array[4]. The flaring emissions from Mrk501 in 1997 and from Mrk421 between 2000 and 2001 were also observed by the Tibet experiment [5, 6]. The Tibet AS experiment is the one which has succeeded in measuring the two-dimensional high-precision large-scale cosmic-ray anisotropy in the northern sky and pointing out a new component of anisotropy in the direction of Cygnus region at multi-TeV energies [7], where the discovery of a TeV diffuse gamma-ray signal was soon claimed by Milagro [8].

However, except Crab Mrk421 and Mrk501, neither the point source nor diffuse gamma-rays have been significantly detected by the Tibet AS array [9–11]. The main reason is that the Tibet AS array is unable to distinguish the primary gamma rays from the primary cosmic-ray nuclei. To improve the sensitivity of gamma ray observation above 10 TeV, we have planned to construct a 10000 m^2 underground muon detector array using water Cherenkov technique, to form the TIBET Ⅲ+MD hybrid array [12, 13]. The Tibet MD array consists of 192 muon detectors with 2.5 m overburden, and each muon detector is a waterproof concrete square pool with 7.2 m in side length and 2.4 m in height. Each pool is equipped with one or two 20 inch-diameter PMTs (HAMAMATSU R3600), depending on the use or not of a large Tyvek bag. The timing and charge information of each PMT is recorded by a trigger signal generated from the surface AS array. The secondary particles in the showers induced by primary gamma rays contain far fewer muons than

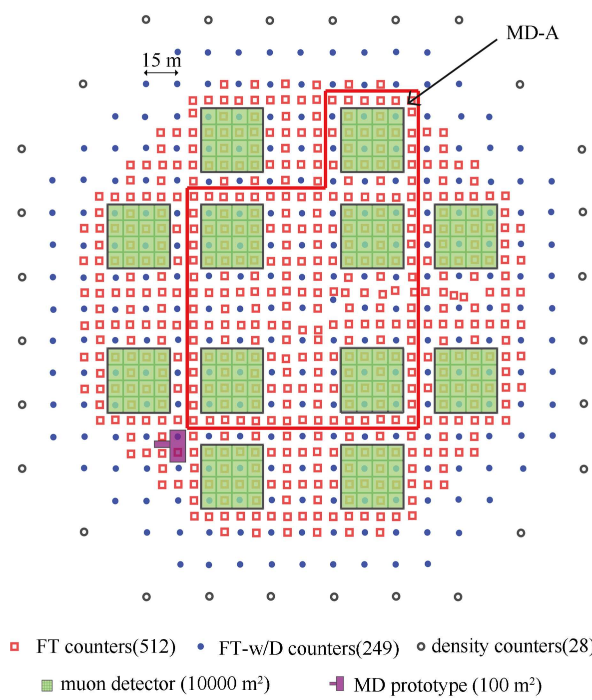

Fig. 1. Schematic view of the Tibet Ⅲ+MD array. Open squares: fast timing counters with a FT-PMT (FT counters); filled circles: FT counters with a D-PMT (FT-w/D counters); open circles: density counters with a D-PMT. The red box indicates MD-I (5 modules, 4500 m^2 in total, 16 pools (4×4) each module), constructed in 2010. Module MD-A is located at the upper right corner of MD-I.

those in the primary hadron induced showers. Therefore, the number of muons in the shower is one powerful parameter in distinguishing the gamma rays from the cosmic ray background. For a full-scale MD configuration [14], Monte Carlo (MC) simulation shows that nearly 99.99% of the cosmic-ray background events can be rejected, while 99% of the primary gamma ray events at 100 TeV can be retained, according to which, a background-free experiment would be realized at an energy above 100 TeV.

In the late fall of 2007, two prototype detectors of approximately 50 m^2 each were constructed under the existing Tibet III array. Each pool was equipped with two PMTs and filled with tap water without any purification or circulation. The typical photoelectron number (N_{pe}) for vertically penetrating muon is 17 [15]. At present, 5 out of 12 modules (MD-I, approximately 4500 m^2 in total, each module has 16 pools) have been constructed and are under installation, as shown in the red box of Fig. 1. Different from the other four modules, the top right module (MD-A) uses a large Tyvek bag filled with high purity water. Details of this technique are described below.

3 The design features of the MD-A

For a water Cherenkov detector, long-term stability of water transparency is very important. Usually, either a water-recycling system or closed container technique is used. For example, the 50 ktons of water in the Super-Kamiokande tank is continuously reprocessed by a water-recycling system [16] and the Pierre Auger Surface Detector is designed to have an operational life span of at least twenty years by using the closed container technique [17]. In MD-A, the latter technique (i.e. enclosing all water in a large bag) is used to stabilize the water quality in the pool. The advantage of this technique not only saves water but is also easy for operation and maintenance.

For this kind of detector, the reflectivity of the bag and the transparency of the water are the most important factors for signal amplitude. We use the Dupont Tyvek 1082D film as the lining of the bag, because this material is flexible, hard wearing, resistant to biological activity and has minimal dissolvable content which might deteriorate the water quality. In addition, this material has outstanding diffuse reflectivity (when the wave length is longer than 350 nm, its diffuse reflectivity is better than 90%) [18]. As the Tyvek film has high air permeability, a three-layer coextruded low-density polyethylene (LDPE) film is laminated outside the Tyvek film. The total thickness of the material is about 375 μm. By using the sealing machine, we successfully produced the windtight large Tyvek bag (7.2 m in side length and 1.9 m in height). To avoid pollution to the Tyvek film, the Tyvek bags are produced in a clean hall and the tools are all cleaned prior to production. Besides, the Tyvek lab coats, hair restraints, gloves and shoe covers are worn during all handling of the film. One Tyvek bag filled with air is shown in Fig. 2. By using such a method, we can prevent water from contamination, and keep good reflection of Cherenkov photons in it. This technique greatly increases the collection efficiency of Cherenkov photons by PMT, although it leads to a longer duration of the output pulse to 800 ns. In other words, to get better muon resolution, we need a wide ADC gate.

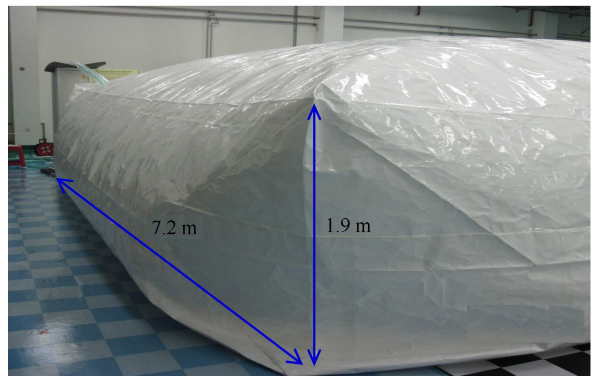

Fig. 2. One of the Tyvek bags (7.2 m in side length and 1.9 m in height) filled with air.

To achieve the longest attenuation length of Cherenkov light and the highest stability of the water, the Tyvek bag is filled with the high-purity water provided by a water purification system. The water purification processes consist of five stages as follows:

1) Pre-processing. To eliminate suspended solids, colloids, organisms, free chlorines and other particles greater than 5 μm, and to ensure that the water fed into reverse osmosis is qualified.

2) Reverse osmosis. It is a filtration method that removes most large molecules and ions from water by applying high pressure to the source water side of a reverse osmosis membrane. The resistivity of the output water is above 30 kΩ·cm.

3) Ultraviolet purification. With a 254 nm UV unit to kill germs in water, and with a 185 nm unit to decompound organic carbon down to 500 ppb.

4) Electro-deionization. It uses ion exchange resins to absorb ions from the diluted water stream and then transport the ions through a pair of ion exchange membranes into a concentrated water stream under the influence of an applied electric field. This process can produce ultra-pure water (resistivity above 10 MΩ·cm).

5) Ultra filter. This step further eliminates particles greater than 0.2 μm.

By using perfluoroalkoxy (PFA) tubing, pools were filled with water with resistivity more than 3 MΩ·cm. Only one HAMAMATSU R3600 PMT is installed in each pool. Fig. 3 shows the schematic view of one pool. Seven pools have been installed and used in a test run operation.

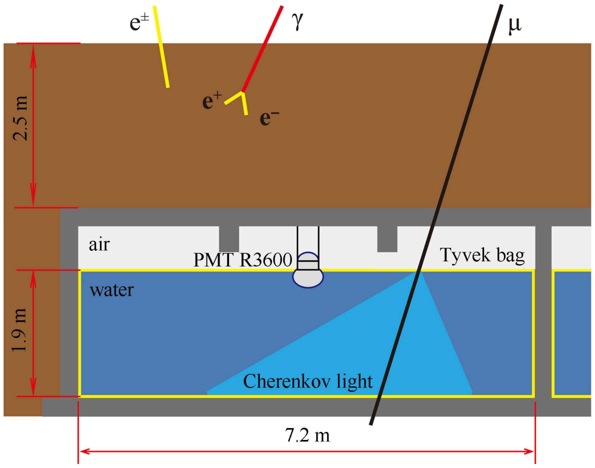

Fig. 3. Schematic view of one pool in MD-A. One 20-inch PMT is mounted at the center of the ceiling and dips into the water to overlook the pool. The bag is filled with high-purity water to keep long-term stability of the water quality.

4 Performance of the MD-A

To study the performance of the detector, we have carried out the following measurements: the signal of single muon events for each pool, the position uniformity, as well as the long-term stability of the detectors.

4.1 The signal of single muon events

To measure the single photoelectron peak, an LED was used as a light source. The driving voltage applied to this LED is generated by a pulse generator, which also feeds a trigger signal to the DAQ system. We change the amplitude and width of the output pulse, to reduce the amount of photons reaching the PMT until the signal-to-noise ratio is approximately 1:9. In this case, the single photoelectron peak is obtained for this PMT [19]. Thus the absolute gain of the PMT at this high voltage can be calculated. Furthermore, after measuring the gain as a function of the applied high voltage, the absolute gain at any high voltage for this PMT can be obtained.

To study the signal of single muon events entering the muon pool, two square scintillation counters of 1 m^2 area with 0.67 m vertical spacing (forming a simple muon telescope) were placed on the ground above the center of the pool. Then, the near vertical incident muon around the center of the pool is selected by requesting a coincident signal in the muon telescope. Fig. 4 shows the measured single muon amplitude spectrum. There is a clear peak around 291 photoelectrons, indicating the average number of measured photoelectrons when one near vertical muon passes through the center of the pool.

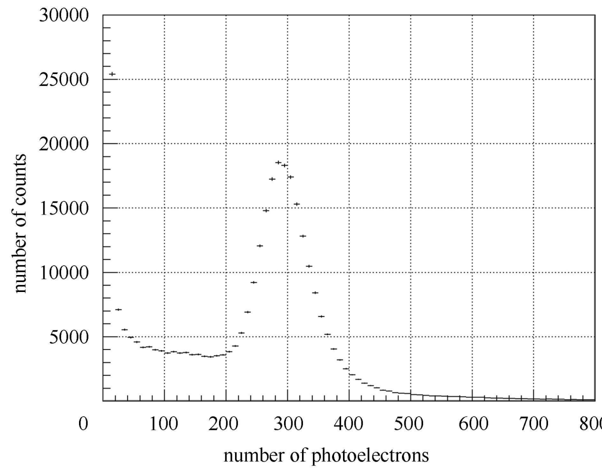

Fig. 4. A clear single muon peak has been observed. The number of collected photoelectrons is obtained for one near vertical single muon entering the center of the pool. The fitted peak position is 291 photoelectrons.

4.2 Position non-uniformity

The position non-uniformity is directly related to the muon number resolution of the detector, since we do not know the incident position in the pool for each muon. To study the position non-uniformity, four positions were selected as shown in Fig. 5(a): the center of the pool (Position A), the side of the pool (Position B), the

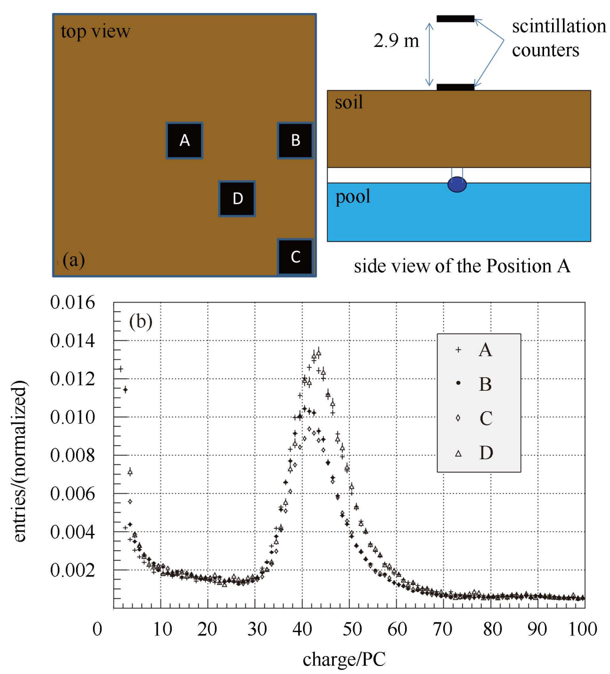

Fig. 5. (a) The schematic view of different positions A, B, C and D; (b) The single muon amplitude spectra for near vertical muon entering at Position A, B, C or D.

corner of the pool (Position C), the middle of A and C (Position D). The above-mentioned muon telescope was placed above the pool on Position A, B, C or D to select the vertical incident muons (the vertical spacing between two scintillation counters is 2.9 m). Fig. 5(b) shows the measured result. The obtained non-uniformity of the muon peak is better than 6%.

4.3 Long-term stability

To study the long-term stability, the single muon amplitude spectrum was continuously monitored with one of the operated pools from 18th September, 2011 to 28th February, 2012. In the operation time of 164 days, the total decay of the peak value is about 13% and the most recent data show that the detector is gradually turning into a stable situation, as shown in Fig. 6. A similar result has been observed by the Auger Surface Detector. The reasons for the decay of signal with time are a convolution of water transparency, Tyvek reflection and electronic response of the detectors [20]. Further study of this behavior is ongoing. Between October and December, other detectors were installed and we stopped the monitor system.

The TIBET III array has a trigger rate of about 1.7 kHz. Considering that the accidental muon rate is about 300 Hz/m^2 at Yangbajing, the rate of accidental coincidence of each trigger in the selected 100ns time window is about 2.5 Hz. So, one hour's data are enough for us to get the single muon peak and to do real-time self-calibration for the muon numbers in each shower.

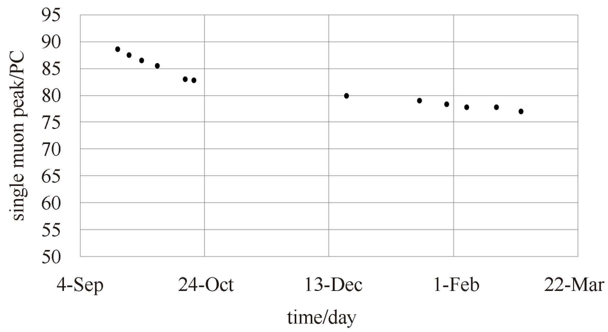

Fig. 6. Long-term stability of the tested Muon DetectorA.

5 Summary

In an attempt to optimize the Tibet MD array, the large Tyvek bag technique is used in MD-A. Up to now, 7 out of 16 pools have been successfully operated and other pools will be ready in the near future. The test run data have shown that the single muon peak can be clearly separated from the detector noise and the detector has good position uniformity. Moreover, the long-term stability of the muon detector is being continuously monitored. Further study of the Tibet III+MD hybrid array is under way.

References

1 Weekes T C et al. ApJ, 1989, **342**: 379–395
2 arXiv: astro-ph/11081435
3 Amenomori M et al. Astrophys. J., 2008, **678**: 1165–1179
4 Amenomori M et al. Astrophys. J., 1999, **525**: 93–96
5 Amenomori M et al. Astrophys. J., 2000, **532**: 302–307
6 Amenomori M et al. Astrophys. J., 2003, **598**: 242–249
7 Amenomori M et al. Science, 2006, **314**: 439–443
8 Atkins R et al. Phys. Rev. Lett., 2005, **95**: 251103
9 Amenomori M et al. Astrophys. J., 2005, **633**: 1005–1012
10 Amenomori M et al. Astrophys. J., 2002, **580**: 887–895
11 Amenomori M et al. Advances in Space Research, 2006, **37**: 1932–1937
12 Amenomori M et al. AIP Conf. Proc., 2008, **1085**: 723–726
13 Amenomori M et al. Journal of Physics: Conference Series, 2008, **120**: 062024
14 The Tibet ASg collaboration, 32nd ICRC, 2011, OG1.5: 0351
15 Sako T K et al. Astropart. Phys., 2009, **32**: 177–184
16 Fukuda S et al. Nucl. Instrum. Methods A, 2003, **501**: 418–462
17 Allekotte I et al. Nucl. Instrum. Methods A, 2008, **586**: 409–420
18 http:// www.dupont.com
19 Tripathi A K et al. NIM A, 2003, **497**: 331–339
20 The PIERRE Auger collaboration. 32nd ICRC, 2011, HE1.4: 0952